A&A 401, 483–489 (2003)
DOI: 10.1051/0004-6361:20030138

Astronomy & Astrophysics

HI observations of nearby galaxies V. Narrow (HI) line galaxies⋆

W. K. Huchtmeier[1], I. D. Karachentsev[2], and V. E. Karachentseva[3]

[1] Max-Plank-Institut für Radioastronomie, Auf dem Hügel 69, 53121 Bonn, Germany
[2] Special Astrophysical Observatory, Russian Academy of Sciences, N.Arkhyz, KChR 369167, Russia
[3] Astronomical Observatory of Kiev University, Observatorna, 3, 04053 Kiev, Ukraine

Received 17 December 2002 / Accepted 22 January 2003

Abstract. In this paper we present new HI observations with high velocity resolution for 104 nearby narrow-line galaxies with half power line widths smaller than 50 km s^{-1} most of which are well approximated by a Gaussian. The *FWHM* line width of 30 of these integrated HI profiles is less than 25 km s^{-1}. We present global parameters of these nearby galaxies and discuss the size dependence, the luminosity dependence, and the dependence of these parameters with the observed line width. Our sample essentially is a subsample of the Local Volume (i.e. galaxies within 10 Mpc) with declinations $\geq -30°$ and only a few galaxies at greater distances. It is described by the following median values of global physical parameters: total absolute blue magnitude $M_{B_t} = -12.85$; linear diameter $A_0 = 1.63$ kpc (this corresponds to the de Vaucouleurs diameter D_{25}); half power line width $W_c = 29$ km s^{-1}; total HI mass $M_{HI} = 2 \times 10^7\ M_\odot$; distance $D = 5.1$ Mpc; HI mass-to-luminosity ratio $M_{HI}/L_B = 0.9\ M_\odot/L_\odot$; total mass-to luminosity ratio $M_t/L_B = 2.9\ M_\odot/L_\odot$.

Key words. galaxies: distances and redshifts – galaxies: dwarf – galaxies: general

1. Introduction

Since the early days of extragalactic spectroscopy it has been known that disk galaxies are dominated by rotation. A spread in observed line widths, i.e. half power line widths of integrated HI profiles or profiles from slit spectroscopy along the major axis of galaxies, from smaller than 50 km s^{-1} to several hundred km s^{-1}, has been observed. However, the number of observed narrow lines has been small in the past. For example, the first systematic catalog of nearby galaxies ($v_0 \leq 500$ km s^{-1}) by Kraan-Korteweg & Tammann (1979) contained 54 galaxies with line widths smaller than 50 km s^{-1} out of 179 galaxies. These numbers do not contain the faint dwarf spheroidals which are not accessible to spectroscopic emission line observations due to their low gas content.

In our HI line search for nearby dwarf galaxy candidates (Paper I to Paper IV) we used a velocity resolution of 6.2 km s^{-1} (or 10.4 km s^{-1} after Hanning smoothing if applied). This resolution resulted from a setup of the autocorrelator optimized for velocity coverage and sensitivity. For the most narrow profiles observed, this yielded only two or three data points per profile, which does not allow a determination of the profile shape. Spikes of radio interference may be mistaken as narrow emission profiles. In order to confirm the detection of these narrow lines and to study their line shapes we repeated HI observations of those galaxies with half power line widths smaller than 50 km s^{-1}. Using a velocity resolution of 1.4 km s^{-1} (2.4 km s^{-1} after Hanning smoothing if applied) we have at least 10 channels with HI emission to describe the line shape; this allows us to simulate the line shape numerically. It turned out that nearly all galaxies in this sample could be approximated by a Gauss-like function. Hence, the Gauss fit was used to derive the systemic velocity and the half power line width for all profiles. All narrow line features observed earlier with coarse velocity resolution could be confirmed and their profile parameters could be measured with much better precision.

In this paper we present the HI observations for 104 narrow-line galaxies in Sect. 2. The data and derived parameters are discussed in Sect. 3. Deriving the total mass will be discussed in Sect. 4 followed by a discussion in Sect. 5.

2. Observations

Observations were performed with the 100-m radio telescope at Effelsberg which has a half power beam width (HPBW) of 9.3′ at the wavelength of 21-cm. A dual channel receiver was followed by a 1024 autocorrelator which was split into four banks of 256 channels each. A bandwidth of 1.56 MHz yielded a channel separation of 1.2 km s^{-1} (a velocity resolution of 1.4 km s^{-1} (2.4 km s^{-1} after Hanning smoothing)). The system noise was around 30 K. Using such a narrow bandwidth resulted in rather flat baselines even in daytime. Observations were performed in the total power mode (ON-OFF) combining the source position with an empty field generally 5 min away in RA.

Send offprint requests to: W. K. Huchtmeier,
e-mail: huchtmeier@mpifr-bonn.mpg.de

⋆ Table 1 is only available in electronic form at
http://www.edpsciences.org

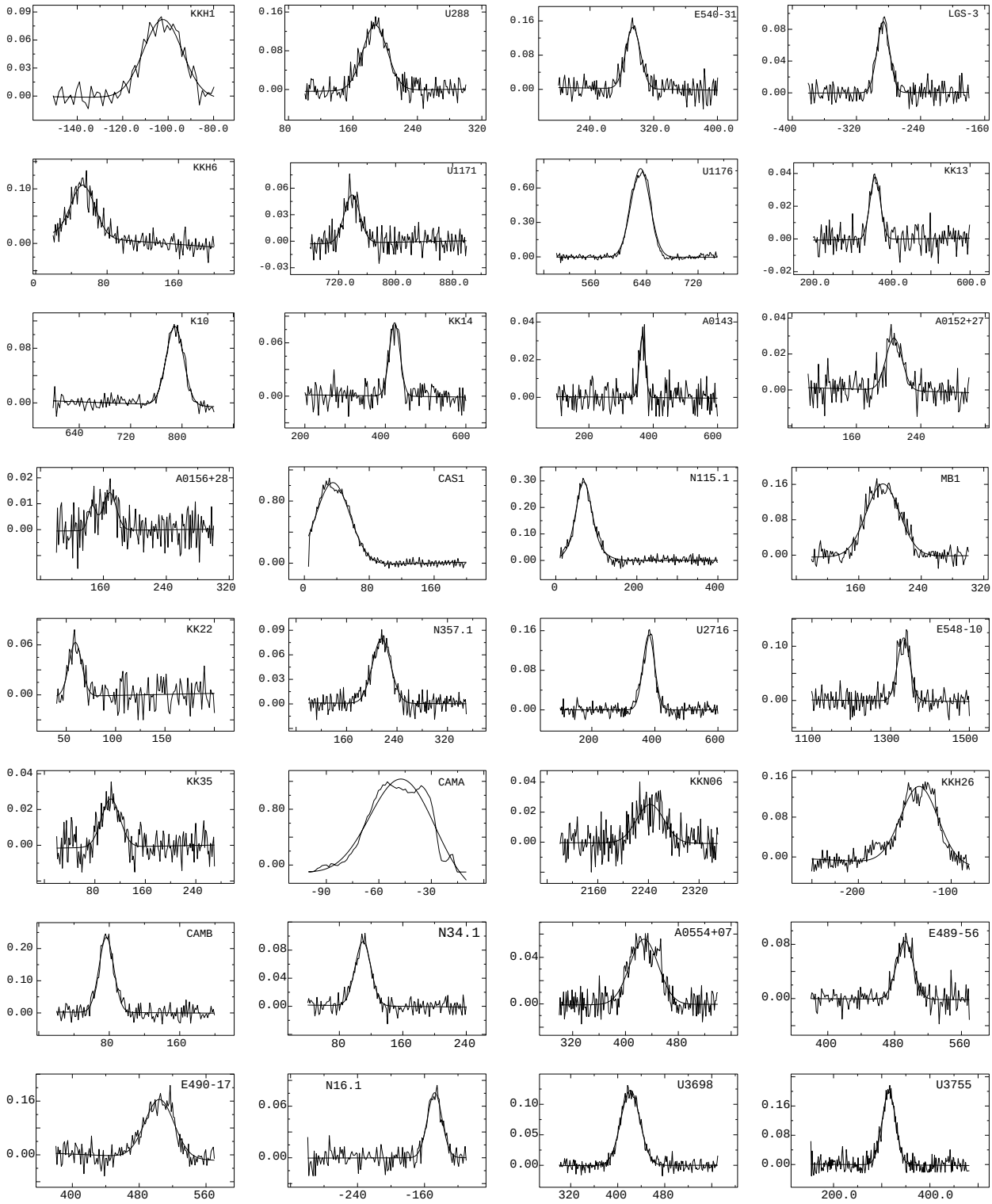

Fig. 1. HI profiles of the dwarf galaxies of our narrow line sample and their Gauss fits. The profiles are arranged in ascending RA starting at the top left corner. The flux scale is in Jy, the heliocentric radial velocity (optical convention) in km s^{-1}. The velocity resolution of most spectra is 1.4 km s^{-1}. The profiles of KK 17, KKSG 6, D564-08, D565-06, KKH51, U5186, KK151, and KK152 have been Hanning smoothed (velocity resolution 2.4 km s^{-1}).

The *Toolbox* software of the MPIfR has been used for the data reduction and presentation. The resulting HI profiles are presented in Fig. 1. In general the signal-to-noise ratio is high for the observed HI profiles. The ON-OFF observing procedure reduced the local HI emission around 0 km s^{-1} to a weak and narrow residual spike. However, for galaxies in the *zone of avoidance* in the Galactic plane the HI emission itself and its changes are stronger than elsewhere. Here the higher

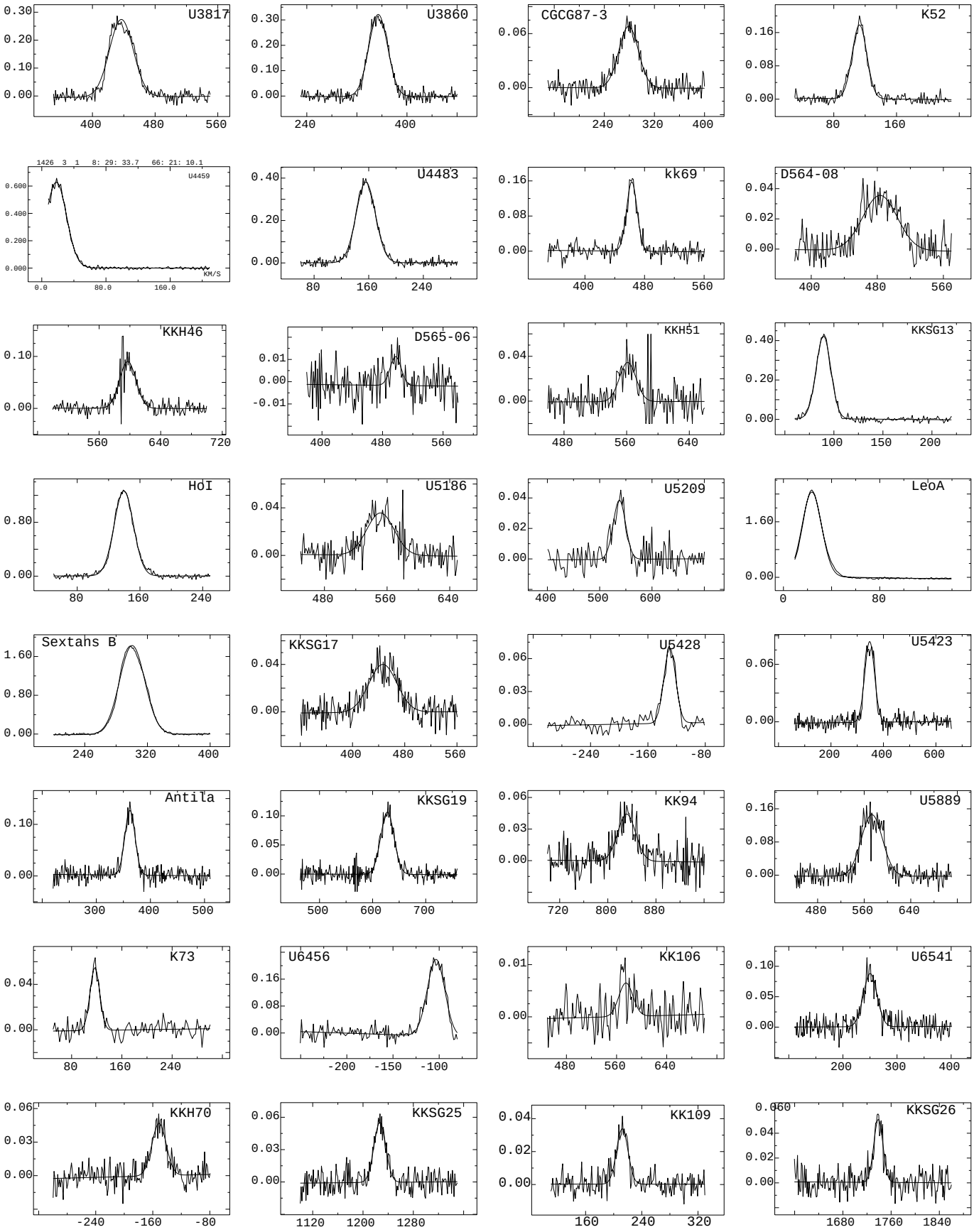

Fig. 1. continued.

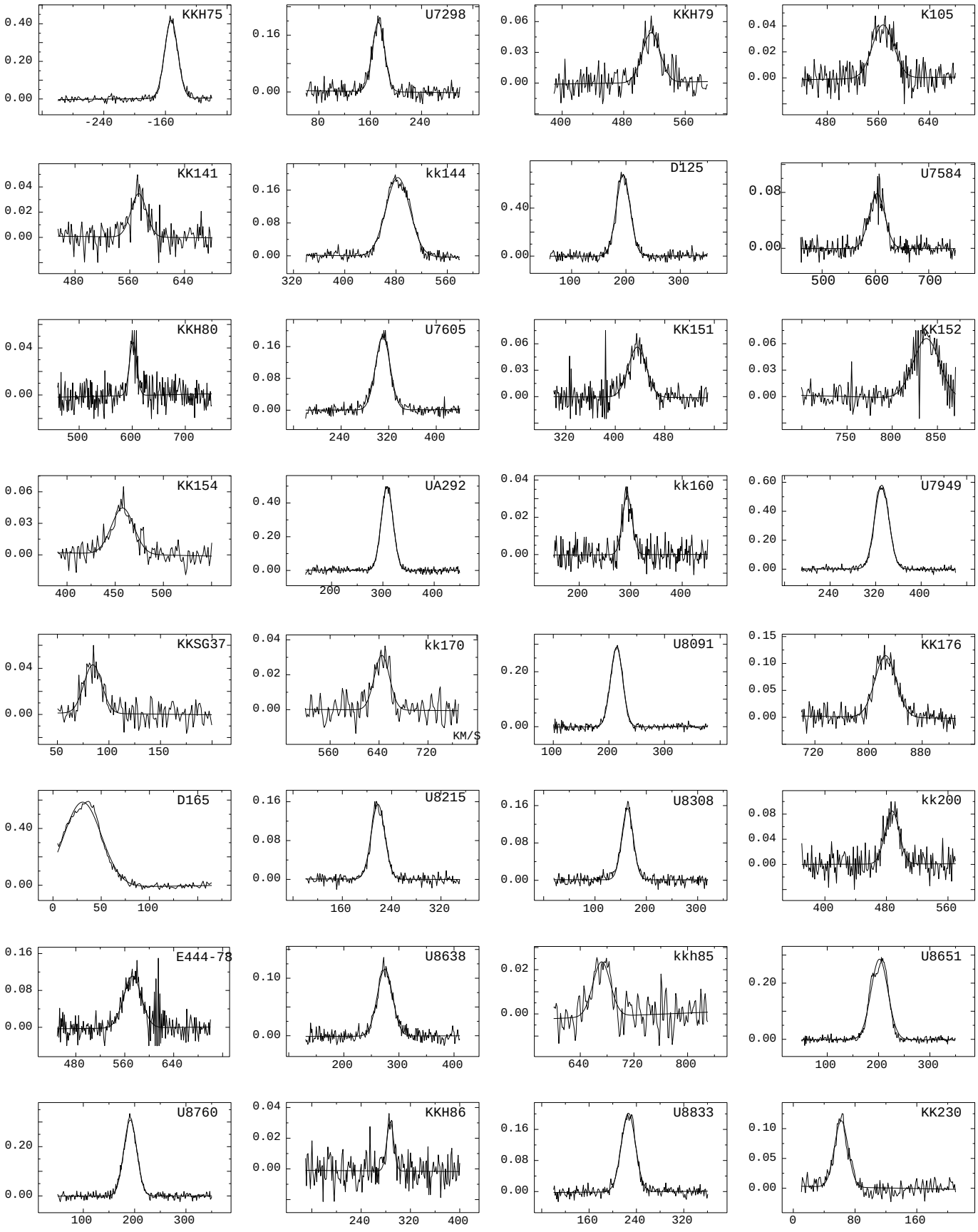

Fig. 1. continued.

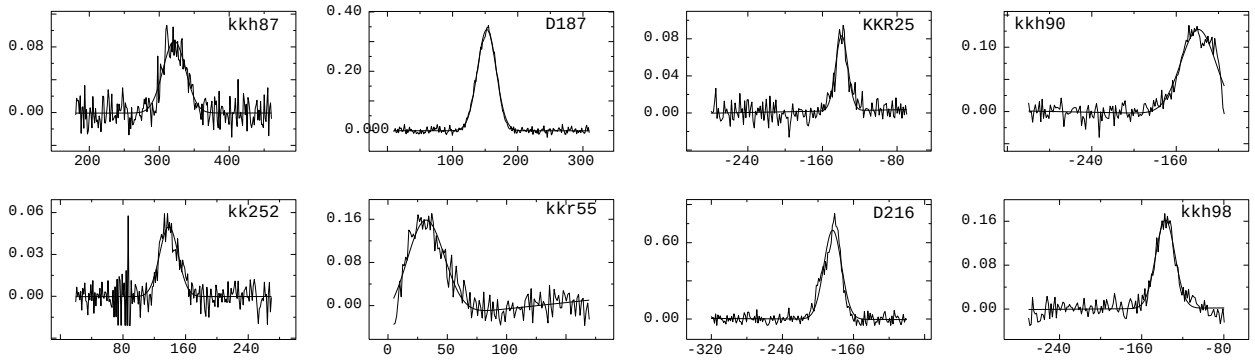

Fig. 1. continued.

velocity resolution helped in separating the HI emission of a given galaxy from the Local HI. There is still some blending of the Local and the galactic HI emission on the low velocity side of a few galaxies like DDO 53, Cassiopeia 1, KKH 12, Leo A, and KKR 55.

Some low level radio frequency interference (RFI) is present at the Effelsberg site producing occasionally spikes in the observed 21-cm band. Even if the RFI occurs within the velocity range of the HI emission of a given galaxy this is not essential for deriving observational parameters, see e.g. KK 148, KK 152, UGC 7584. These spikes generally disappear after Hanning filtering.

3. The data

In Table 1 we give the galaxy name in Col. 1 followed by the 1950.0 position in Col. 2. The integrated HI flux (line integral in Jy km s^{-1}) in Col. 3 is followed by the maximum flux density and its error in mJy (Col. 4), the heliocentric systemic velocity $V_{\rm h}$ and its error (Col. 5), and the half power line width and its error (Col. 6). The distance and a code for the method used is given in Col. 7; here the code (with the estimated error of the method in parantheses) means c = cepheids (10%), r = red giant branch stars (12%), s = surface brightness fluctuations (15%), m = group membership (20%), b = bright stars (25%), t = Tully-Fisher relation (30%), h = Hubble distance (ca. 30%) assuming $H_0 = 70$ km s^{-1} Mpc^{-1}. The absolute magnitude follows in Col. 8 (the total blue apparent magnitude was corrected for Galactic absorption following Schlegel et al. 1998). The relative HI content normalized by the total blue luminosity, $M_{\rm HI}/L_B$ in solar units, follows in Col. 9. The integrated HI mass and the total mass were calculated as in Paper III, i.e.

$$M_{\rm HI}/M_\odot = 2.356 \times 10^5\ D^2\ LI_{\rm HI}, \quad (1)$$

where D is the distance in Mpc and $LI_{\rm HI}$ the line integral (integrated HI flux) in Jy km s^{-1}, and

$$M_{\rm t} = 0.83 \times 10^4\ a\ W^2_{\rm c,50}\ D, \quad (2)$$

where a is the optical diameter (D_{25}) in arcmin, D the distance in Mpc and $W_{\rm c,50}$ the observed half power line width corrected for instrumental broadening but not for inclination.

The "total" mass-to-luminosity ratio in solar units M/L_B follows in Col. 10. Comments are given in Col. 11.

We admitted galaxies with line widths slightly larger than 50 km s^{-1} when this limit was within 3 times the r.m.s. error of the line width. Tifft & Huchtmeier (1990) compared HI data from the 100-m radio telescope at Effelsberg and the 91-m radio telescope at Green Bank and discussed systematic errors due to the observing procedure and the data reduction software. For narrow profiles they deduce systematic errors smaller than 0.1 km s^{-1}, the same is true for pointing errors. Values in Cols. 4 to 6 of Table 1 are the result of a Gauss-fit procedure with stable results in the presence of noise.

Viewing the HI profiles in Fig. 1 it is obvious that most of them are fitted well by a Gaussian curve. A few exceptions are noticed among the brighter galaxies in our sample. Asymmetries with respect to a Gauss curve are observed for the galaxies UGC 1176, Cassiopeia 1, DDO 165 (UGC 8201), and in the faint Pegasus dwarf irregular galaxy DDO 216. This might partially be due to structure in the HI distribution.

Significant deviations from Gaussian curves were also noted in KK41 (CamȦ), UGC 5889, UGC 8651 where we observe a rudimentary double peaked profile typical of spiral galaxies.

For most galaxies the integrated HI flux given in Col. 3 of Table 1 should be the correct value as the median apparent blue diameter of this sample is only 1.2 arcmin, which is small compared to the main beam (9.3 arcmin HPBW). The range of apparent blue diameter is from 0.4 arcmin to 5.1 arcmin. There are nine galaxies with apparent blue diameter larger than 2.4 arcmin, up to about 5 arcmin for the Pegasus dwarf irregular, Leo A, and Sextans B. For these galaxies our observations will not provide the total integrated HI flux (Broeils & Rhee 1997).

Only few of the galaxies in this sample have been observed before with higher velocity resolution and higher spatial resolution. VLA observations of LGS-3 (Young & Lo 1997) with a velocity resolution of 1.28 km s^{-1} and a spatial resolution from ∼36″ to ∼64″ yield an HI extend of ∼6 arcmin. Hence the tapering of the Effelsberg beam yields an integrated HI flux about 30% lower (i.e. 1.7 Jy km s^{-1}) compared to 2.7 Jy km s^{-1} observed with the VLA. The agreement of the derived systemic radial velocities is excellent, -286.5 ± 0.3 km s^{-1} and -286.5 ± 0.25 km s^{-1} (VLA).

VLA observations of faint dwarf galaxies by Lo et al. (1993) yield similar integrated fluxes for the galaxies in common except for Leo A for which they derive an HI extent

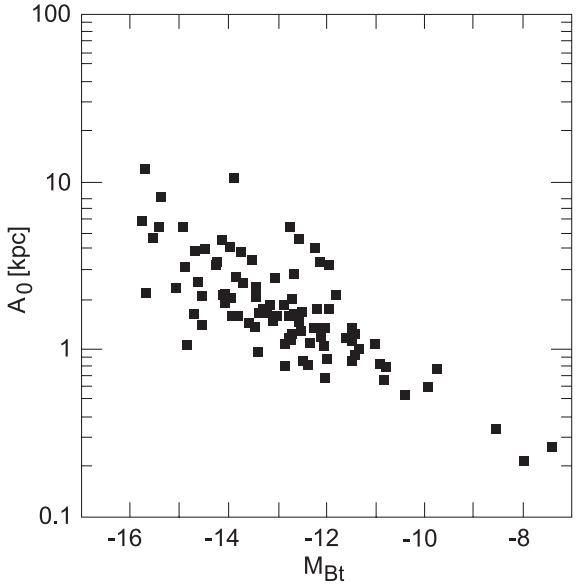

Fig. 2. The linear extent A_0 in kpc (corresponding to the de Vaucouleurs diameter D_{25}) is plotted versus the absolute blue magnitude M_{Bt} of the galaxies of our sample. It is obvious that the smaller the galaxies, the fainter they are.

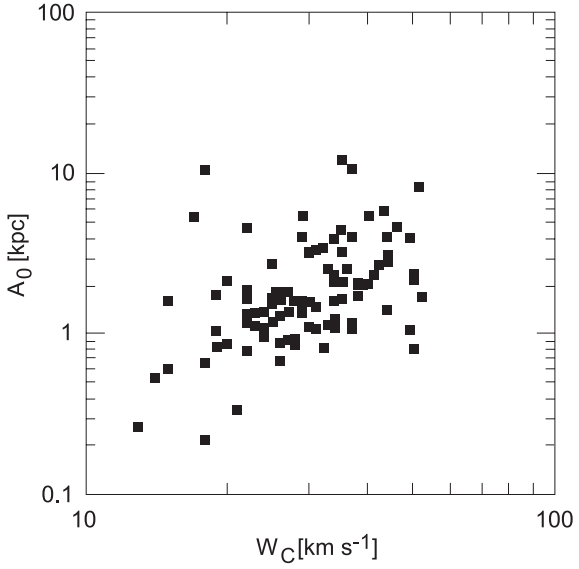

Fig. 3. The linear extent A_0 is plotted versus the HI half power line width W_c (corrected for intrumental broadening). On average, small galaxies are characterized by narrow lines.

of ∼7 arcmin and an HI flux of 68.3 Jy km s^{-1} compared with the 48.3 Jy km s^{-1} observed with the 100-m radio telescope.

4. Total mass

In their study of the *HI structure of nine intrinsically faint dwarf galaxies* based on VLA observations, Lo et al. (1993) found that tiny dwarf galaxies fainter than about −13 M_{Bt} show little sign of rotation, typically $V_{rot} \sin i \leq 5$ km s^{-1}. In these galaxies the rotational velocity is less than the three dimensional random velocity dispersion. More massive dwarfs, like Holmberg I and Cas 1, definitely are dominated by rotation. In the case of a system with chaotic motion dominating rotation, such as the HI in faint dwarf galaxies, one can apply the Virial theorem on the mass determination. Here we assume the HI gas in a steady state within the gravitational potential.

From their HI maps Lo et al. could derive the velocity dispersion at different points in the galaxy and measure the HI extent to derive the total mass applying the Virial theorem. For the present data we only have the integrated HI profiles and cannot separate rotation from the velocity dispersion. We therefore normalized the expression for the total mass based on the square of the observed line width W_c[km s^{-1}], the angular extent a [′] of the galaxy and its distance D [Mpc] by the total masses derived by Lo et al. (1993) which yields M_{VT} in solar masses:

$$M_{VT} = 1.48 \times 10^4 \; a \; D \; W_c^2. \qquad (3)$$

This global value for the total mass is uncertain by a factor of 2 at least. In view of this error and the uncertainty of the inclination we used the same relation for the total mass we have been using in previous papers of this series (see Eq. (2)).

5. Discussion

Given the relative resolution into stars of their optical image and their different optical radial velocities eight (i.e. KKH 1, KKH 26, KKH 37, KKSG13, KKH 70, KKH 75, KKSG 37, and KKH 90) of the 104 observed HI profiles – mostly with negative radial velocities – have been considered to be of local origin (Galactic foreground), leaving 96 galaxies to be discussed further.

Most of the galaxies in our sample are classified as dwarf irregulars. There are a few late-type spirals and five dwarf spheroidals classified as dSph or dSph/Irr. 30 galaxies have line widths smaller than 25 km s^{-1}.

Global parameters like M_{Bt}, M_{HI}, M_t, and A_0 correlate with each other as known from many studies of spiral and irregular galaxies. In Fig. 2 we present a plot of the linear diameter versus absolute blue magnitude. This shows the range of size and luminosity of galaxies in our sample.

For the tiny galaxies in our sample it is impossible to correct for inclination as inclinations derived from axial ratios are extremely uncertain for galaxies with “irregular” structure. In addition the intrinsic axial ratio probably increases with decreasing mass; this value is not well defined either.

For the larger galaxies in our sample the inclination may be derived from the shape of the HI distribution assuming rotation to be the dominant motion, as in Cas1. Here the mass-to-luminosity ratio M_t/L_B increases by a factor of 2 when the inclination is taken into account.

It is evident that very narrow line widths of the integrated HI profiles are associated with small and faint galaxies. This is demonstrated in Figs. 3 to 5 where the line width W_c is plotted versus the linear extent A_0 (Fig. 3), the absolute blue magnitude M_{Bt} (Fig. 4), and the total HI mass M_{HI} (Fig. 5) of the galaxies in our sample. The definite correlation of the line width with the other global parameters yields the conclusion that the galaxies with the smallest line widths in our sample are on average also

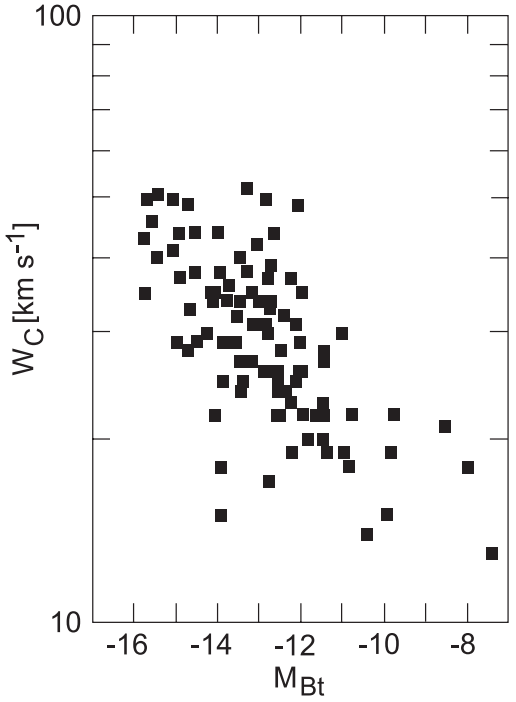

Fig. 4. The HI half power line width W_c (corrected for instrumental broadening) is plotted versus absolute blue magnitude M_{Bt} for the galaxies in our narrow line sample. On average faint galaxies have narrow line widths.

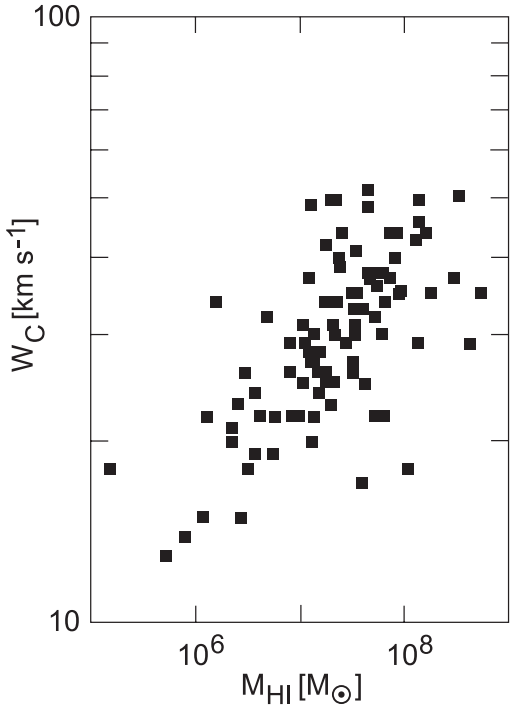

Fig. 5. The HI half power line widths W_c (corrected for instrumental broadening) is plotted versus the integrated HI mass M_{HI} of the galaxies in our narrow line sample. On average galaxies with narrow lines have small HI masses.

the smallest in linear size (Fig. 3), the faintest in absolute magnitude (Fig. 4) and those with the smallest HI mass (Fig. 5).

The total mass-to-light ratio M_t/L_B is not correlated with inclination, linar extent A_0, HI mass M_{HI} or total mass M_t.

Since the earliest compilation of nearby galaxies (Kraan-Korteweg & Tammann 1979) the number of nearby galaxies has doubled and the number of gas-rich galaxies at the faint end of the luminosity function increased by about the same factor. As the actual sensitivity for faint galaxies (optically and in HI) is limited, we are by far not complete for the local volume ($\leq$10 Mpc).

6. Conclusion

In this paper we presented HI observations with high velocity resolution for 96 galaxies with line widths smaller than 50 km s^{-1}. These dwarf galaxies have small apparent blue diameters (median: 1.2 arcmin). The median values for linear extent (A_0 = 1.63 kpc), absolute blue magnitude ($M_{Bt} = -12.85$), and the integrated HI mass ($M_{HI} = 2 \times 10^7\ M_\odot$) show they are dwarfish galaxies, indeed. Most profiles (except 5) could be well approximated by a Gaussian function. The correlations between global parameters (M_{Bt}, A_0, M_{HI}, M_t, and W_c that have been determined for spiral galaxies are seen to extend to the faint end of the galaxy luminosity function.

Acknowledgements. This paper is based on observations with the 100-m radio telescope of the MPIfR (Max-Planck-Institut für Radioastronomie) at Effelsberg. We have made extensive use of the NASA/IPAC Extragalactic Database (NED, which is operated by the Jet Propulsion Laboratory, Caltech, under contract with the National Aeronautics and Space Administration), and the Digitized Sky Survey (DSS–1) produced at the Space Telescope Science Institute under U.S. Goverment grant NAG W–2166. Our project is partially supported by DFG grant No 436 RUS 113/470/0.

References

Broeils, A. H., & Rhee, M.-H. 1997, A&A, 324, 877
Huchtmeier, W. K., Karachentsev, I. D., & Karachentseva, V. E. 2000, A&AS, 141, 469 (Paper II)
Huchtmeier, W. K., Karachentsev, I. D., & Karachentseva, V. E. 2001, A&A, 377, 801 (Paper IV)
Huchtmeier, W. K., Karachentsev, I. D., Karachentseva, V. E., & Ehle, M. H. 2000, A&AS, 141, 469 (Paper I)
Karachentsev, I. D., Karachentseva, V. E., & Huchtmeier, W. K. 2001 A&A, 366, 428 (Paper III)
Kraan-Korteweg, R. C., & Tammann, G. A. 1979, Astron. Nachr., 300, 181
Lo, K. Y., Sargent, W. L. W., & Young, K. 1993, AJ, 106, 507
Makarov, D. I., & Karachentsev, I. D. 2003, A&A, submitted
Marvel, K. B., & Wilcots, E. M. 2000, AJ, 120, 2038
Sargent, W. L. W., Sancisi, R., & Lo, K. Y. 1983, ApJ, 265, 711
Schlegel, D. J., Finkbeiner, D. P., & Davis, M. 1998, ApJ, 500, 525
Tifft, W. G., & Huchtmeier, W. K. 1990, A&AS, 84, 47
Young, L. M., & Lo, K. Y. 1997, ApJ, 490, 710